

The Study of Crystallization Dynamics of Amorphous Precursor $\text{Fe}_{70}\text{Mo}_5\text{Cr}_4\text{Nb}_6\text{B}_{15}$ Alloy

KONRAD GRUSZKA*, JAKUB RZACKI, MARCIN NABIALEK

Institute of Physics, Faculty of Production Engineering and Materials Technology, Czestochowa University of Technology,
19 Armii Krajowej Str., 42-200 Czestochowa, Poland

The paper presents the results of studying the dynamics of the crystallization process for the samples subjected to three separate processes of isothermal heating with three different energy in the process. For this purpose, a series of samples prepared in the form of a ribbon of an amorphous structure, as confirmed from X-ray diffraction were then subjected to a controlled annealing. The research of samples after heat treatment revealed the presence of different crystalline phases that are characterized by different nucleation energies.

Keywords: XRD, nanocrystallization, crystallization dynamics, melt spinning

The process of crystallization is of great importance for the final properties of the material subjected to this procedure [1-6]. From the parameters of this process it will depend on what the final atomic structure material will have. Also whether and to what extent this structure will be ordered, and will this structure be defected or have some and inhomogeneities, etc. At the same time, the atomic structure of the material has a huge impact on its various properties [7-15] which results directly from the kind of interaction between neighboring atoms, and those situated a little further. Apart from the crystallization process of the material, a large impact on the final structure has the precursor, on which the heat treatment procedure is carried out [16-18]. Precursor predetermines some properties, since it stands as a base, on which further actions are made. It can also be a certain limit, for eg. if one wish to obtain a specific structure, not realizable in a given case. This implies that more universal precursor gives the greater possibility of obtaining diversity of structures and properties of the target material.

It is well known that the crystallization is a process resulting in the decrease of the total energy of the material. However, to obtain crystallites composed of more than one ingredient in the volume of the material, these ingredients should have a negative heat of mixing [19], otherwise segregation of components will occur, preventing the formation of multi-component phases. These conditions can be satisfied by amorphous materials. Because long-range ordered structure in amorphous materials is not observed and local fluctuations in their composition and density are very common [20-24], despite their short-range order, the structure has rather more random in character. For this reason, amorphous materials are considered to be metastable, meaning that in terms of energy they do not reach a global minimum, and are located only in some instable higher energy state. Over time, material is seeking for the lowest possible energy. Metastable state is characterized by the fact that it is sufficient to provide a finite and usually small amount of energy, in eg. in the the form of heat, which allows to overcome the local potential barrier resulting in change of their structure to more stable. For this reason, and for the reasons mentioned above, amorphous materials are

excellent precursor for further thermal treatment in order to obtain a material with specific structure made of expected crystalline phases. The temperature distribution for this type of material can be modeled using the finite element method [26-29].

In this work we present the study results for samples of the composition $\text{Fe}_{70}\text{Mo}_5\text{Cr}_4\text{Nb}_6\text{B}_{15}$, in the as quenched state and after three independent thermal annealing processes.

Experimental part

Material preparation procedure

Samples in the form of polycrystalline ingots were prepared with ingredients of high purity. First, components were premixed and then melted using an arc furnace under protective atmosphere of argon. In order to ensure the best possible homogeneity of the material ingots were repeatedly reversed, and re-melted. Thus obtained polycrystalline ingot was then melted in induction furnace and in the process of rapid cooling on the copper roll sample was solidified to a ribbon with a width of 1 cm and a thickness of 20 micron (precursor). From the ribbon several fragments with a length of 20 mm were cutted, which were separately subjected to the heat treatment processes, maintaining the parameters as homogeneous as possible. For this purpose fragments of the precursor were placed in quartz capillary tubes, flushed several times with argon, followed by the removal of gas from within the capillaries. Then they were sealed and heat treated in a computer-controlled resistance furnace. The heat treatment temperature was selected on the basis of previously performed DSC measurement (DSC NETZSCH STA 449F1) on the pure precursor. In order to determine the atomic structure of the precursor, XRD studies using the BRUKER D8 Advance diffractometer equipped with Cu tube (characteristic radiation of wavelength $\lambda = 1.5418 \text{ \AA}$) in the 2θ angle ranging from 20° to 110° with measuring step of 0.19° . The remaining samples were subjected to three different processes of isothermal annealing at different temperatures, 800 K, 895 K, 920 K for the samples #1, #2 and #3 respectively. In all cases the annealing time was fixed to 30 min. Then after treatment, the structure of samples were investigated with X-ray diffraction. The

* email: kgruszka@wip.pcz.pl

Sample	Annealing temperature [K]	Annealing time [min]	Vacuum pressure [Pa]
#0	-	-	-
#1	800	30	1.33×10^{-3}
#2	895	30	1.33×10^{-3}
#3	920	30	1.33×10^{-3}

Table 1
ANNEALING PROCESS PARAMETERS

parameters of the production process are contained in table 1.

The paper also presents the results obtained by Rietveld refinement. Quantitative Rietveld phase refinement was performed using Fullprof software. The fit was performed using: scale factor, unit cell parameters refinement and additional background parameters. A shifted background polynomial with 5 parameters was used to refine the background signals. A pseudo-Voigt function described the peaks shape. Due to the symmetry of peaks additional parameters associated with the asymmetry were not taken into account. All fittings were obtained for the final reduced χ^2 lower than 4.

Results and discussions

Figure 1 presents the results of XRD measurement for sample of the precursor (in the as quenched state)

As can be seen by analyzing the diffraction pattern (fig. 1) on the chart is visible only a wide blurred halo whose maximum falls at 2θ angle of about 43 degrees. There are no visible narrow peaks in the whole angular range, which proves the absence of the long-range topological arrangement in the volume of sample, proving no crystal planes. The nature of the diffraction pattern indicates a complete amorphous content of the investigated material.

Figure 2 shows the diffraction patterns of the samples subjected to isothermal annealing process.

Analyzing figure 2 it can be concluded that all three samples had experienced at least partial crystallization of the material. On the diffractogram (fig 2. a) for the sample

#1 it can be seen that there is also an amorphous halo, similar to that shown in figure 1, and quite broad peaks appeared contained between the 2θ angles of 46 - 55° and 75 - 83°. The presence of a fuzzy broad peak is characteristic for samples with an amorphous structure and the simultaneous presence of peaks with low intensities derived from the crystalline phase in this case shows the coexistence of both types of phases in the sample volume. The relatively high intensity of the amorphous halo in respect to the peak intensity and a relatively large half width of peaks suggests the presence of crystalline phase grains of relatively small (nanometer) size of the crystallites which are embedded in an amorphous matrix constituting larger volume of sample. The indexing of phases occurring in the diffraction patterns (fig. 2) was carried out using the COD database [30]. The parameters of identified phases are shown in table 2.

In order to estimate the size of the crystal grains present in the sample, the Scherrer method was utilized, and the results of this analysis are shown in table 3.

As can be seen by analyzing table 1, there is a general relationship in the crystallite size with respect to the annealing temperature of the sample. The effect of the grain enlarging with increasing temperature can be explained by the fact that, although the heating time was constant, higher energy delivered to the specimen is accelerating the crystallization front movement by increasing the diffusion of atoms in its local environment.

For samples #2 and #3 character of the diffraction pattern is different, peaks present in the diffractogram are

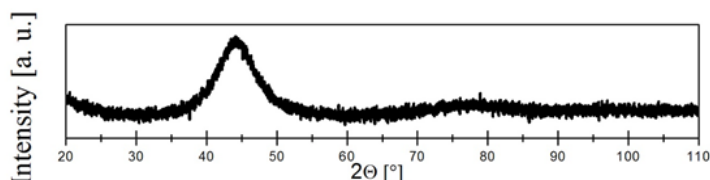


Fig. 1. X-ray diffraction patterns of $\text{Fe}_{70}\text{Mo}_5\text{Cr}_4\text{Nb}_6\text{B}_{15}$ alloy in the as-quenched state

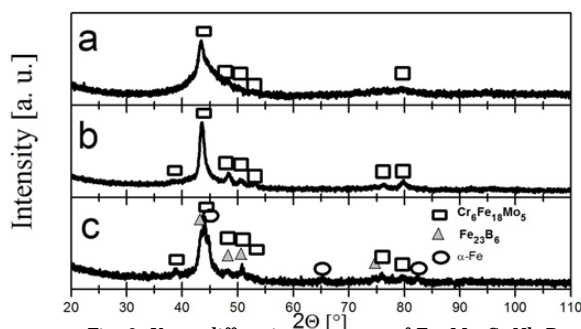


Fig. 2. X-ray diffraction patterns of $\text{Fe}_{70}\text{Mo}_5\text{Cr}_4\text{Nb}_6\text{B}_{15}$ alloy after annealing for 0.5 h at 800 K (a), 895 K (b) and 920 K (c).

Phase	Space group (number)	Symmetry	Cell parameters [Å]
$\text{Cr}_6\text{Fe}_{18}\text{Mo}_5$ [31]	I-43m (217)	Cubic	8.920
Fe_{23}B_6 [32]	Fm-3m (225)	Cubic	10.671
$\alpha\text{-Fe}$ [33]	Im-3m (229)	Cubic	2.868

Table 2
PROPERTIES OF IDENTIFIED CRYSTALLINE PHASES

Sample	Identified crystalline phase	Sherer grain size [nm]
#1 (800 K)	$\text{Cr}_6\text{Fe}_{18}\text{Mo}_5$	58
#2 (895 K)	$\text{Cr}_6\text{Fe}_{18}\text{Mo}_5$	94
#3 (920 K)	$\text{Cr}_6\text{Fe}_{18}\text{Mo}_5$	111
	Fe_{23}B_6	109
	$\alpha\text{-Fe}$	124

Table 3
THE GRAIN SIZE OF THE PHASE DETERMINED ON THE BASIS OF SHERRER ANALYSIS

much more intense than in the case of sample #1. The increased intensity of the peaks also indicates increase in the volume of the grains formed at the cost of an amorphous matrix.

In order to determine the parameters of phases elementary cells and their relative share, samples #2 and #3 were subjected to the Rietveld analysis. The results of this analysis are shown in table 4.

Sample	Phase	Cell parameter a [Å]	Share [%]
#2	$\text{Cr}_6\text{Fe}_{18}\text{Mo}_5$	8.852	100
#3	$\text{Cr}_6\text{Fe}_{18}\text{Mo}_5$	8.824	57
	Fe_{23}B_6	10.6772	31
	$\alpha\text{-Fe}$	2.866	12

Table 4
RIETVELD
REFINEMENT
RESULTS

As can be seen by analyzing the data from table 4, for the sample treated at the highest temperature (#3), phase with largest percentage is $\text{Cr}_6\text{Fe}_{18}\text{Mo}_5$, second largest part of the share is a newly formed Fe_{23}B_6 phase. For samples #1 and #2, the only observed phase is Fe_{23}B_6 . The increase in annealing temperature (so increase of delivered energy) causes crystallization of two additional phases Fe_{23}B_6 and $\alpha\text{-Fe}$, despite that the difference in annealing temperature between samples #2 and #3 is relatively small. The size of grains for $\text{Cr}_6\text{Fe}_{18}\text{Mo}_5$ and Fe_{23}B_6 in sample #3 are similar, while the grain of $\alpha\text{-Fe}$ phase are only slightly bigger (table 3), what can suggest similar crystallization dynamics for those two phases. In the other hand, although grains of $\alpha\text{-Fe}$ phase are the biggest, the share of this phase in respect to remaining ones is the lowest.

The fact that volume fraction of $\text{Cr}_6\text{Fe}_{18}\text{Mo}_5$ phase is the highest is probably caused by longer exposition to temperature.

The volume fraction of $\text{Cr}_6\text{Fe}_{18}\text{Mo}_5$ phase is the highest because in the process of isothermal annealing even at lower temperature the growth of this phase was observed. Thus, due to lower energy necessary for crystallization, the share of this phase largest. The above analysis also shows that because of almost three times the share of Fe_{23}B_6 in relation to the $\alpha\text{-Fe}$, it should have a lower energy needed for crystallization. In addition, the reason may well be in the local depletion of iron due to growth of $\text{Cr}_6\text{Fe}_{18}\text{Mo}_5$ phase, and a large boron content in the sample, which may cause the growth of Fe_{23}B_6 phase was preferred. Also, it should be noted that the crystal seeds of all identified phases were already in the precursor and thus their maximal amount does not have to be the same.

By the analysis of the data in table 4, it can be seen that for sample #3 and #4 cell size of the phase $\text{Cr}_6\text{Fe}_{18}\text{Mo}_5$ in both cases is slightly lower than that reported in [29, 30], similar for the Fe_{23}B_6 phase for which the calculated cell size is also slightly smaller [31, 32]. At the same time, these differences are so small that this estimation may lie in the margin of error.

Conclusions

In this work we studied crystallization process of $\text{Fe}_{70}\text{Mo}_5\text{Cr}_4\text{Nb}_6\text{B}_{15}$ alloy samples submitted to isothermal annealing of amorphous precursor. We showed, that starting from the very same precursor sample a completely different material can be obtained, only by slightly varying crystallization process parameters, such as temperature. This small change will often result with completely different crystallization dynamics, leading to different properties of material. We also calculated several parameters including share of crystalline phases and estimated their grain sizes.

It was shown, that the latter is connected with temperature of annealing demonstrating its simple relation.

References

- 1.R.B. POND JR., R. MADDIN, Transactions of the Metallurgical Society of the American Institute of Mechanical Engineers (SAUS) **245**, 1969, p. 2475.
- 2.K. GRUSZKA, M. NABIALEK, K. BLOCH, J. OLSZEWSKI, *Nukleonika* **60**, 2015, p. 23.
- 3.MCHENRY, M. C., WILLARD, M. A., & LOUGHLIN, D. E., *Prog. Mater. Sci.*, **44**, 1999, p. 291.
- 4.PIETRUSIEWICZ, P., NABIALEK, M., SZOTA, M. DOSPIAL, M., BLOCH, K., BUKOWSKA, A., GRUSZKA, K., *Arch. Metall. Mater.* **59**, 2014, p. 659.
- 5.P. PIETRUSIEWICZ, K. BLOCH, M. NABIALEK, S. WALTERS, *Acta Phys. Pol. A* **127**, 2015, p. 397.
- 6.K. GAWDZINSKA, K. BRYLL, D.NAGOLSKA, Influence of Heat Treatment on Abrasive Wear Resistance of Silumin Matrix Composite Castings, *Arch. Metall. Mater.*, **61**, no. 1, 2016, p. 177.
- 7.BLOCH, K., *Rev.Chim.(Bucharest)*, **68**, no. 10, 2017, p. 2413.
- 8.GAWDZINSKA K., *Archives Of Metallurgy And Materials*, **58**, no. 3, 2013, p. 659.
- 9.K. BLOCH, M. NABIALEK, P. PIETRUSIEWICZ, J. GONDRO, M. DOSPIAL, M. SZOTA, K. GRUSZKA, *Acta. Phys. Pol. A* **126**, 2014, p. 108.
- 10.A. INOUE, X.M. WANG, W. ZHANG, *Rev. Adv. Mater. Sci.*, **18**, 2008, p. 1.
- 11.MINCIUNA, M.G., VIZUREANU, P., *Metalurgia International*, **18**, Special issue 6, 2013, p. 123.
- 12.SANDU, A.V., CIOMAGA, A., NEMTOI, G., BEJINARIU, C., SANDU, I., *Microscopy Research And Technique*, **75**, no. 12, 2012, p. 1711.
- 13.RAMBU, A.P., SIRBU, D., SANDU, A.V., PRODAN, G., NICA, V., *Bulletin of Materials Science*, **36**, no. 2, 2013, p. 231.
- 14.VIZUREANU, P., PERJU, M.C., GALUSCA, D.G., NEJNERU, C., AGOP, M., *Metalurgia International*, vol. XV, no. 12, 2010, p. 59.
- 15.TUGUI, C.A., NEJNERU, C., GALUSCA, D.G., PERJU, M.C., AXINTE M., CIMPOESU N., VIZUREANU P., *Journal of Optoelectronics and Advanced Materials*, **17**, no. 11-12, 2015, p. 1855.
- 16.W.H. WANG, C. DONG, C.H. SHEK, *Mater. Sci. Eng. R*, **44**, 2004, p. 45
- 17.Q. ZHENG, *Rev. Adv. Mater. Sci.*, **40**, 2015, p. 1.
- 18.P. DUWEZ, R. H. WILLENS, Transactions of the Metallurgical Society of the American Institute of Mechanical Engineers (SAUS), **227**, 1963, p. 362
- 19.A. BRENNER, D.E. COUCH, E.K. WILLIAMS, *J. Res. Natl. Bur. Stand.* **44**, 1950, p. 109.
- 20.P. PIETRUSIEWICZ, M. NABIALEK, M. DOSPIAL, K. GRUSZKA, K. BLOCH, J. GONDRO, P. BRAGIEL, M. SZOTA, Z. STRADOMSKI, *J. Alloys Comp.* **615**, 2014, p. S67.
- 21.J. GONDRO, J. SWIERCZEK, J. RZCKI, W. CIURZYNSKA, J. OLSZEWSKI, J. ZBROSZCZYK, K. BLOCH, M. OSYRA, A. LUKIEWSKA, *J. Magn. Magn. Mater.* **341**, 2013, p. 100.
- 22.A. P. THOMAS, M.R.J. GIBBS, *J. Magn. Magn. Mater.*, **103**, 1992, p. 97.
- 23.S.N. KAUL AND P.D. BABU, *Phys. Rev. B*, **45**, 1992, p. 295.
- 24.S.N. KAUL AND CH.V. MOHAN, *J. Phys: Condens. Matter* **3**, 1991, p. 2703
25. L.A. DOBRZANSKI, A. SLIWA, W. SITEK, *Surf. Eng. 5 ISEC*, 2006, p. 26.
26. A. SLIWA, B. BONEK, J. MIKULA, *Appl. Surf. Sci.*, **388**, 2016, p. 174
- 27.L.W., ZUKOWSKA, A., SLIWA, J., MIKULA, M. BONEK, W. KWASNY, M. SROKA, D., PAKULA, *Arch. Metall. Mater.*, **61**, 2016, p. 149
- 28.A. SLIWA, J., MIKULA, K. GOLOMBEK, T. TANSKI, B. BONEK, W. KWASNY, Z. BRYTAN, *Appl. Surf. Sci.*, **388**, 2016, p. 281
- 29.S. GRAZULIS, D. CHATEIGNER, R. T. DOWNS, A. T. YOKOCHI, M. QUIRÓS, L. LUTTEROTTI, E. MANAKOVA, J. BUTKUS, P. MOECK, A. LE BAIL, *J. Appl. Cryst.*, **42**, 2009, p. 726.
- 30.J. S. KASPER, *Acta Metallurgica*, **2**, 1954, p. 456.
- 31.T. NAKAMURA, H. KOSHIBA, M. IMAFUKU, A. INOUE, E. MATSUBARA, *Materials Transactions*, **43**, No. 8, 2002, p. 1918.
- 32.K. LEJAEGERE, V. VAN SPEYBROECK, G. VAN OOST, S. COTTENIER, *Critical Reviews in Solid State and Materials Sciences*, **39**, no. 1, 2014, p. 1

Manuscript in received: 15.10.2017